

Influence of raw materials morphology on properties of magnesia-spinel refractories

Jacek Szczerba^{a,*}, Zbigniew Pędzich^a, Małgorzata Nikiel^b, Dominika Kapuścińska^{a,b}

^a AGH, University of Science and Technology, Faculty of Materials Science and Ceramics,
al. Mickiewicza 30, 30-059 Cracow, Poland

^b Magnesite Works “Ropczyce” S.A., Poland

Available online 27 June 2006

Abstract

The work concerns magnesia-spinel refractories (MSP) used in cement industry. These materials replace magnesia chromite refractories due to environment protection. The paper summarizes results of investigation on influence of raw materials on final properties of magnesia-spinel products. In experiments sintered or fused magnesia, and fused spinel were used. Clinkers differ in chemical composition and morphology. Grain composition of mixtures was calculated on the basis of modified Andraesen curve according to Dinger and Funk's model.

Essential influence of clinker morphology on final properties of refractories was established. Porosity and pore size distribution in materials determine their strength and gas permeability. Relations between these parameters allow controlling the final properties of products in a wide range. © 2006 Elsevier Ltd. All rights reserved.

Keywords: Refractory materials; Spinel

1. Introduction

The type of refractories containing spinel $\text{MgO} \cdot \text{Al}_2\text{O}_3$ (MA) named nowadays magnesia-spinel products (MSP)¹ was patented first time in 1932 in Austria. This material was manufactured by introduction of alumina into the magnesia mixes.² During the firing alumina reacted with periclase and MA spinel was formed. Due to significant differences of thermal expansion coefficients of spinel ($8\text{--}9 \times 10^{-6} \text{ }^\circ\text{C}^{-1}$) and periclase ($13\text{--}15 \times 10^{-6} \text{ }^\circ\text{C}^{-1}$), the material with net of microcracks was formed. Such microstructure assured higher thermal shock resistance in a new material. These materials did not find wider applications due to poor quality magnesia clinkers used for production. They have high level of impurities and low density. These products were pushed out for a long time by magnesia chromite products—much cheaper and easier in manufacturing. In magnesia chromite refractories microstructure with presence of microcracks were reached by combination of magnesia clinker and chrome ore which was spinel phase carrier.

Increase of ecological problems connected with utilisation of cements containing soluble Cr^{6+} ions and used up magne-

sia chromite products caused repeated interesting in magnesia-spinel products (MSP). This technology was strongly investigated in Japan 30 years ago.³ This trend was exported to European countries.^{4,5} Development of MSP materials was possible due to elaboration of spinel clinker (MA) production technology in Japan. This clinker is a fundamental raw material for MSP products.

The name spinel is parallel used as a name of chemical compound – MgAl_2O_4 and as a name of the group of chemical compounds with general formula – AB_2O_4 , where A and B describe respectively, bi- and tri-valent metals. Stoichiometric spinel contains 28.2 wt.% of MgO and 71.8 wt.% of alumina. It's melting temperature is $2135 \text{ }^\circ\text{C}$.⁶ It is only the one chemical compound in $\text{MgO}\text{--}\text{Al}_2\text{O}_3$ binary system (Fig. 1). In practice, refractory semi-products manufactured in this system could contain periclase and spinel, only the spinel or spinel and corundum obtained by firing or melting.⁷ The types of spinel manufactured on the $\text{MgO}\text{--}\text{Al}_2\text{O}_3$ system base could be:

- almost stoichiometric, utilized for production of different type of refractories;
- with MgO exceed ($>28 \text{ wt.}\%$), utilized mainly in cement industry;
- with Al_2O_3 exceed ($>70 \text{ wt.}\%$), utilized for low cement concretes for steel works or special type products (i.e. well block).

* Corresponding author. Tel.: +48 1248 6172501.

E-mail address: jszczerb@uci.agh.edu.pl (J. Szczerba).

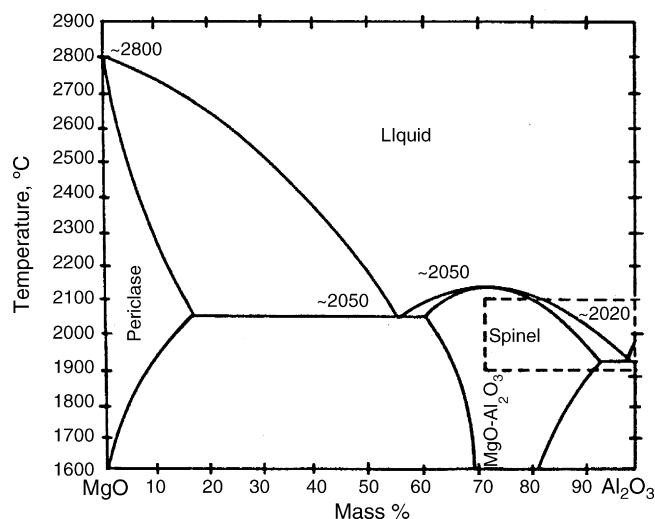


Fig. 1. The MgO–Al₂O₃ binary system.⁶

In cement industry MSp products containing up to 20 wt.% of spinel clinker (fired and/or melted) found the application.^{8–10} Using of this material assures a full reaction of alumina with magnesia.⁷ A presence of free alumina in clinker promotes corrosion processes—alumina and calcium can create calcium aluminates with low melting point.

The raw materials for these spinel synthesis is alumina (achieved by Bayer method), different kinds of bauxite and sometimes brucite or slug from plasma melting of nonferrous metals and calcined magnesia or fired one, achieved from natural magnesites, or by chemical preparation of chemical compounds containing magnesia (i.e. see water–synthetic magnesia).

It is common knowledge that products achieved from the mixture of natural magnesia clinker and fused spinel show better resistance for alkalis than these achieved from sea water magnesia and sintered spinel.¹¹ They work better in furnaces with high alkali concentration, large amount of liquid phase in clinker and in furnaces with non-stable coating. In the case of redox conditions in sintering zone of cement furnaces, the MSp products with low Fe content (<0.5 wt.% of Fe₂O₃) are used.

Success in the cement industry caused that MA containing materials were utilizing also in steel works. The development in metallurgical technology and processing of many operations in ladles caused increase of metal temperatures and prolonged soaking time in the tundish. Such conditions were too hard for alumina-silicate linings. In 1988, alumina-silicate linings were replaced with success by concretes containing sintered or fused corundum and MA spinel in the matrix. Other “metallurgical” applications of MA spinel nowadays are linings of induction furnaces and metal melting crucibles. The spinel is also utilized as a component of the material for sliding gate plate.

A potential, still narrow utilized, application of MA spinel containing materials is glass industry. They could be used as middle areas of glass tank regenerators, which is subjected for temperature changes and chemical treatment of alkali and sulphur. The MA spinel containing products show better resistance for such environments than widely used MC materials.

Modern technologies of cement clinker production widely utilize alternative raw materials and fuels. This causes much more intensive interaction between furnace atmosphere and refractory lining.^{11–13} The reduction of furnace atmosphere containing alkali oxides, SO_x, Cl ions, CO₂, CO and others could be reached by porosity decrease of used basic refractory materials. A new types of materials containing calcium zirconate,^{14,15} hercynite,^{16,17} galaxite¹⁸ or oxide additives (ZrO₂, Fe₂O₃, TiO₂, SiO₂, Al₂O₃) which modify chemical and mineralogical composition^{10,19,20} are not fully satisfactory. The long durability of basic refractories mainly depends on minimal changes of temperature and technological condition in the furnace. In such condition, what is confirmed by industry experience, magnesia-spinel products are the best solution.¹²

Presented paper described the influence of the used magnesia type (sintered or fused) with different chemical composition and physical properties on final properties of magnesia-spinel product. The content of fused spinel was constant. These investigations were focused on limitation of influence of liquid clinker phase and furnace atmosphere on refractory durability. The goal of the work was to achieve magnesia-spinel products with low gas permeability, open porosity and profitable pore structure. The influence of magnesia clinker or fused magnesia on product densification was determined in dependence on grain distribution coefficient *n* (according to Dinger and Funk²¹) and maximum grain size.

2. Experimental

Presented investigations were focused on the clinker morphology influence of the final properties of magnesia-spinel products. During investigation different raw magnesia (sintered or fused) and fused spinel were used. Clinkers have different chemical composition and physical properties. Fused spinel has chemical composition similar to stoichiometric one—MgO – 28.2% and Al₂O₃ – 71.8%. Properties of raw materials were collected in Table 1.

The pore size distribution of raw materials are showed in Fig. 2. Both of sintered magnesia (clinker 1 and 2) are characterized by the high amount of pores below 10 μm in comparison with fused magnesia and fused spinel. The major part of pores in fused spinel is bigger than 35 μm.

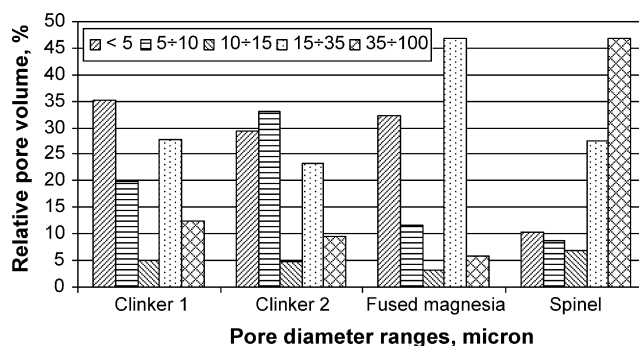


Fig. 2. Diagram collecting of pore size distribution of raw materials (at indicated ranges).

Table 1
Properties of raw materials

Raw material	Clinker 1	Clinker 2	Fused magnesia	Spinel
Chemical composition (mass%)				
MgO	95.21	98.12	96.72	26.38
CaO	0.49	0.89	1.98	0.27
SiO ₂	1.29	0.26	0.68	0.03
Fe ₂ O ₃	2.18	0.48	0.37	0.19
Al ₂ O ₃	0.29	0.10	0.07	72.96
CaO/SiO ₂ (mol)	0.38	3.67	3.1	–
Physical and mineralogical properties				
Bulk density (g/cm ³)	3.11	3.28	3.41	3.35
Apparent porosity (%)	10.8	2.2	3.1	3.0
Crystal size (average) (μm)	25–70	120–150	500–600	>1000

Investigations were conducted on products which were combination one type of clinker (sintered magnesia) (Types Ia and Ib, Types IIa and IIb) or fused magnesia (Types IIIa and IIIb). Types Ia, IIa, IIIa products contain 92 mass% of one kind of clinker or fused magnesia and 8 mass% of spinel. Types Ib, IIb, IIIb products contain 82 mass% of one kind of clinker or fused magnesia and 18 mass% of spinel. Type II and III products contained clinker 2 or fused magnesia with low amount of Fe₂O₃ (respectively 0.48 and 0.37 mass%) and Type I products contained clinker 1 higher Fe₂O₃ level (2.18 mass%). The grain size distribution of all types of products was fitted according to Dinger and Funk's model²¹ for different grain distribution coefficient n equal to 0.15, 0.22, 0.30 and 0.37. The maximum grain size was changed from 3 to 6 mm (for clinker or fused magnesia) and minimal grain size was 0.0001 mm. The maximum grain size for spinel was 3 mm.

The magnesia-spinel refractory mixes with 3 mass% addition of sulphite waste liquor additive were formed in cylindrical samples of 50 mm in diameter and 50 mm in height under 160 MPa. The effect of forming pressure on magnesia-spinel properties were described only for samples Type II with different amount of spinel and for the grain size distribution coefficient n equal 0.30 under 120, 160 and 200 MPa.

Samples were dried at 120 °C and fired in furnace with electric heating element. Type I samples were fired at 1600 °C, and Type II and III samples at 1650 °C with 5 h soaking time at maximum temperature. The effect of forming pressure on magnesia-spinel properties were investigated only for samples

Types Ia and IIa with the same amount of spinel for grain size (8 mass%) and for the grain size distribution coefficient n equal 0.30. They were fired at temperatures 1550, 1600, 1650 and 1600, 1650, 1700 °C, respectively.

For fired samples following properties were determined:

- bulk density according to EN 993-1,
- open porosity according to EN 993-1
- cold crushing strength according to EN 993-5,
- gas permeability according to EN 993-4,
- pore size distribution by mercury porosimetry with Carlo Erba Micropore 140 and Porosimeter 2000 equipment.

3. Results

Tables below collect properties of samples—bulk density, apparent porosity, gas permeability, cold crushing strength and volumetric firing shrinkage. These data are completed with diagrams illustrating pore size distribution at indicated ranges (35–100, 15–35, 10–15, 5–10 and below 5 μm).

3.1. Effect of firing temperature and forming pressure on the MSp properties

Properties of samples Types Ia and IIa prepared for grain size distribution $n = 0.30$ at function of temperature are presented in Table 2.

Table 2
Physical properties of samples with 8 mass% of spinel as a function of firing temperature

	Sample					
	Type Ia			Type IIa		
	1550 °C ^a	1600 °C	1650 °C	1600 °C	1650 °C	1700 °C
Bulk density (g/cm ³)	2.88	2.88	2.90	2.92	2.93	2.98
Apparent porosity (%)	19.7	18.4	17.9	16.2	15.8	13.8
Gas permeability (nPm)	2.98	3.25	3.98	3.15	3.18	3.24
Cold crushing strength (MPa)	50.8	54.5	72.1	63.7	64.9	73.7
Volumetric firing shrinkage, ΔV (%)	1.0	1.9	2.1	0.8	1.2	1.4

^a Firing temperature.

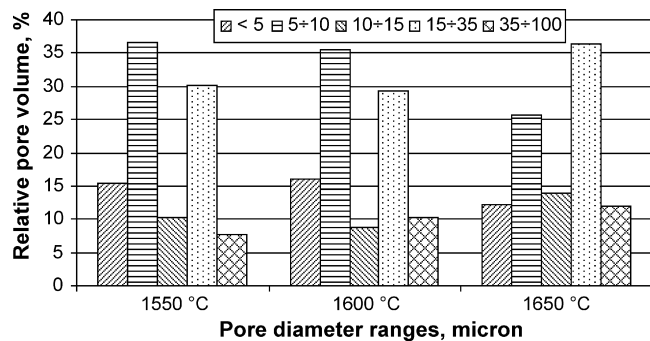


Fig. 3. Diagram collecting of pore size distribution of Type I samples (at indicated ranges).

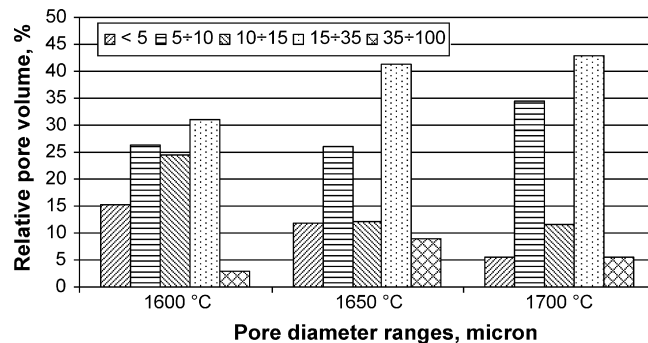


Fig. 4. Diagram collecting of pore size distribution of Type II samples (at indicated ranges).

Samples Type Ia fired at temperature 1550 and 1600 °C have similar properties (density and porosity) but shrinkage was significantly different. Samples Type Ia fired at temperature 1650 °C showed the lowest porosity and the highest strength. The strength increase exceeded 30% and it was achieved with shrinkage similar to the sample fired at 1600 °C. The level of densification of samples slightly increased with sintering temperature increase. Volume fraction of pores bigger than 15 μm increased insignificantly (Fig. 3). It caused that also gas permeability increased slightly (Table 2).

Samples of Type IIa fired at 1600 °C, 1650 °C show similar properties: bulk density, porosity, gas permeability, cold crushing strength and volumetric shrinkage. Samples fired at 1700 °C reached much lower porosity (of course shrinkage was higher). During sintering at the highest temperature pores below 5 μm were eliminated. Volume fraction of bigger pores (5–10 and 15–35 μm) increased (Fig. 4). Such pore size distribution caused slight increase of gas permeability (Table 2) with densification increase.

Properties of samples Type IIa and IIb prepared for grain size distribution coefficient $n = 0.30$ depending on forming pressure are given in Table 3. Both types of samples show the same tendencies of property changes with forming pressure increase. The apparent density of samples slightly increases but the cold crushing strength increases distinctly. The open porosity and gas permeability decrease with forming pressure increase. Both types of products show similar firing shrinkage ($\sim 1\%$). It is worth to notice that samples formed under higher pressure reach profitable pore size distribution with higher content of pores

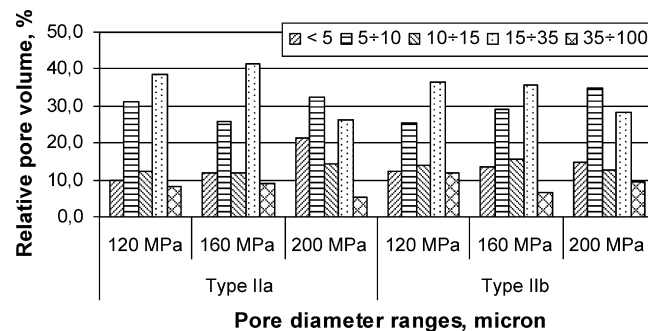


Fig. 5. Diagram collecting of pore size distribution of Type II samples in dependence on forming pressure (at indicated ranges).

smaller than 15 μm . This is a source of their lower gas permeability (see Table 3 and Fig. 5).

On the basis of presented results, one forming pressure 160 MPa was fixed for investigations of influence of the maximum grain size on final magnesia-spinel product properties. The firing temperature was 1600 °C for Type I samples (on the clinker 1 basis) and 1650 °C for Type II samples (on the clinker 2 basis).

3.2. Effect of grain size distribution on the properties of MS_p manufactured on the basis of sintered magnesia

Properties of samples Type I and II for different grain size distribution coefficient n values and for different maximum grain of clinker sizes are presented in Tables 4–6. The higher amount of fine grains fraction in mixes (low n values) leads to the increase

Table 3
Physical properties of samples for different forming pressure and $n = 0.30$

	Sample					
	Type IIa			Type IIb		
	120 MPa ^a	160 MPa	200 MPa	120 MPa	160 MPa	200 MPa
Bulk density (g/cm^3)	2.92	2.93	2.95	2.87	2.90	2.94
Apparent porosity (%)	16.1	15.8	15.4	17.7	16.9	15.9
Gas permeability (nPm)	4.18	3.18	2.61	4.98	4.14	2.96
Cold crushing strength (MPa)	47.4	64.9	74.9	58.8	63.0	62.9
Volumetric firing shrinkage, ΔV (%)	1.2	1.2	1.0	1.0	1.0	0.8

^a Forming pressure.

Table 4
Physical properties of Type Ia samples with 8 mass% of spinel

	Clinker 1 up to					
	5 mm		3 mm		4 mm	6 mm
	<i>n</i> = 0.15	<i>n</i> = 0.22	<i>n</i> = 0.30	<i>n</i> = 0.30	<i>n</i> = 0.30	<i>n</i> = 0.30
Bulk density (g/cm ³)	2.85	2.87	2.88	2.87	2.88	2.89
Apparent porosity (%)	19.5	19.1	18.4	18.5	18.3	18.5
Gas permeability (nPm)	1.96	2.54	3.25	2.55	2.63	3.46
Cold crushing strength (MPa)	60.3	59.7	54.5	67.8	66.7	63.5
Volumetric firing shrinkage, ΔV (%)	2.0	1.6	1.8	1.8	1.6	1.4

n: grain size distribution coefficient.

Table 5
Physical properties of Type IIa samples with 8 mass% of spinel

	Clinker 2 up to					
	5 mm		3 mm		4 mm	6 mm
	<i>n</i> = 0.15	<i>n</i> = 0.22	<i>n</i> = 0.30	<i>n</i> = 0.30	<i>n</i> = 0.30	<i>n</i> = 0.30
Bulk density (g/cm ³)	2.89	2.92	2.93	2.92	2.94	2.97
Apparent porosity (%)	17.4	16.2	15.8	16.2	15.6	14.1
Gas permeability (nPm)	1.67	2.38	3.18	2.15	2.20	3.44
Cold crushing strength (MPa)	85.8	69.3	64.9	92.1	90.0	78.1
Volumetric firing shrinkage, ΔV (%)	1.2	1.0	1.2	1.3	1.2	1.1

n: grain size distribution coefficient.

of open porosity and cold crushing strength. The slight decrease of the apparent density is accompanied with distinct decrease of gas permeability. It reaches values lower than 2 nPm for products with 8 mass% of fused spinel (for *n* = 0.15) (see Tables 4 and 5). The pore size distribution in dependence on *n* value for Type IIa and IIb samples are showed in Figs. 6 and 7. Type II samples

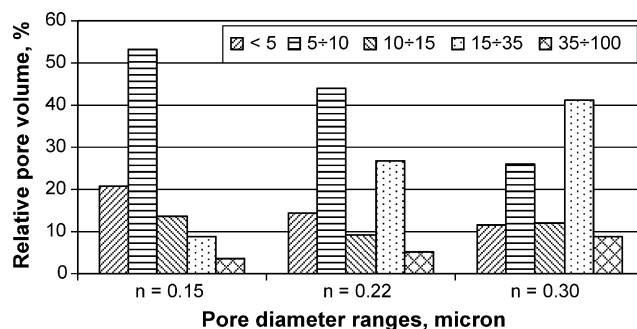


Fig. 6. Diagram collecting of pore size distribution of Type IIa samples in dependence on *n* value (at indicated ranges).

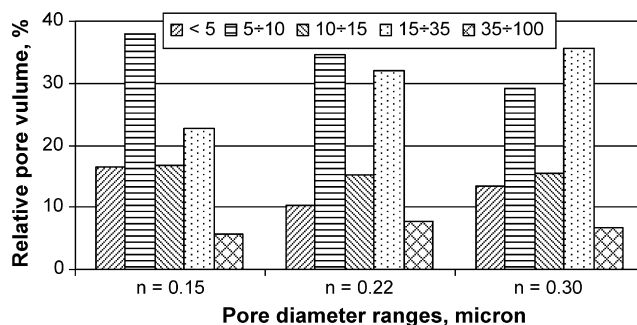


Fig. 7. Diagram collecting of pore size distribution of Type IIb samples in dependence on *n* value (at indicated ranges).

containing also 8% and 18% of fused spinel with low *n* value are characterized by pores smaller than 10 μm , mainly. It concerns distinctly products with 8% of spinel content. Samples prepared with higher *n* value, containing of higher amount of fused spinel have the major part of pores bigger than 10 μm . It causes higher gas permeability in samples with higher amount of fused spinel. The comparison of pore size distribution of Types I and II for *n* = 0.30 and for maximum grain size in the mix equal 5 mm are presented in Fig. 8. These samples show similar pore size distribution. It is probably influenced by pore size distribution of used magnesita clinker (see Fig. 2).

Samples of Types I and II show similar firing shrinkage. It decreases for mixes with small amount of the finest grains.

A Type Ia products for *n* = 0.30 and maximum grain size of 3–6 mm have almost the same properties, excluding the gas permeability. Its value for samples with maximum grain size 3 and 4 mm is about 2.5 nPm and for samples with maximum grains

Table 6
Physical properties of samples with 18 mass% of spinel for maximum grain size of clinkers 1 and 2 up to 5 mm

	Sample					
	Type Ib			Type IIb		
	<i>n</i> = 0.15	<i>n</i> = 0.22	<i>n</i> = 0.30	<i>n</i> = 0.15	<i>n</i> = 0.22	<i>n</i> = 0.30
Bulk density (g/cm ³)	2.88	2.88	2.88	2.89	2.90	2.90
Apparent porosity (%)	19.0	18.8	18.7	17.6	17.2	16.9
Gas permeability (nPm)	2.39	3.25	4.19	2.24	2.76	4.14
Cold crushing strength (MPa)	59.8	51.7	47.7	69.3	74.3	63.0
Volumetric firing shrinkage, ΔV (%)	1.5	1.4	1.4	1.2	1.0	1.0

n: grain size distribution coefficient.

Table 7

Physical properties of Type IIIa samples with 8 mass% of spinel and maximum grain size of fused magnesia up to 5 mm

	Firing temperature (°C)							
	1650				1700			
	<i>n</i> =0.15	<i>n</i> =0.22	<i>n</i> =0.30	<i>n</i> =0.37	<i>n</i> =0.15	<i>n</i> =0.22	<i>n</i> =0.30	<i>n</i> =0.37
Bulk density (g/cm ³)	2.93	2.98	3.02	3.06	2.95	2.99	3.03	3.05
Apparent porosity (%)	17.2	15.8	14.6	13.7	16.8	15.5	14.3	13.6
Gas permeability (nPm)	3.1	3.5	4.6	6.1	3.9	4.4	4.8	6.3
Cold crushing strength (MPa)	92.6	92.2	79.2	78.6	101.2	99.6	92.4	80.6
Volumetric firing shrinkage, ΔV (%)	1.3	0.8	0.7	1.0	1.4	1.1	0.8	1.2

n: grain size distribution coefficient.

Table 8

Physical properties of Type IIIb samples with 18 mass% of spinel and maximum grain size of fused magnesia up to 5 mm

	Firing temperature (°C)							
	1650				1700			
	<i>n</i> =0.15	<i>n</i> =0.22	<i>n</i> =0.30	<i>n</i> =0.37	<i>n</i> =0.15	<i>n</i> =0.22	<i>n</i> =0.30	<i>n</i> =0.37
Bulk density (g/cm ³)	2.92	2.93	2.98	3.0	2.92	2.95	2.97	3.0
Apparent porosity (%)	17.7	17.2	16.0	15.4	17.7	16.8	16.0	15.4
Gas permeability (nPm)	4.2	4.6	6.2	7.9	4.4	5.7	7.5	8.1
Cold crushing strength (MPa)	58.2	57.1	51.7	48.6	55.3	51.5	50.4	46.0
Volumetric firing shrinkage, ΔV (%)	0.9	0.5	0.5	0.6	1.4	1.1	1.0	0.8

n: grain size distribution coefficient.

5 and 6 mm about 3.4 nPm (see Table 4). The influence of the high grain size limit on product properties is distinctly visible for Type IIa samples (Table 5). They show high gas permeability and apparent density when the grain size limit is high (5 or 6 mm). Their open porosity distinctly decreases. Also the crushing strength decreases, but still its value is on the level accepted for this class of products. In samples manufactured with grains of 6 mm, when compared with samples with smaller maximum grain size, pores bigger than 15 μm dominate (see Fig. 9). It is connected with lower content of the finest grains in basic mixes when the maximum grain size increases.

3.3. Effect of grain size distribution on the properties of MSp manufactured on the basis of fused magnesia

For better characteristic of the influence of raw materials properties and their morphology on magnesia-spinel products

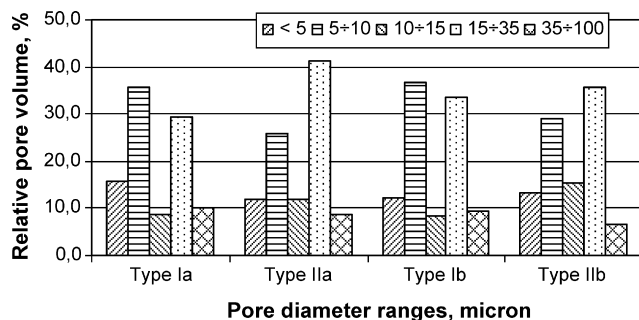
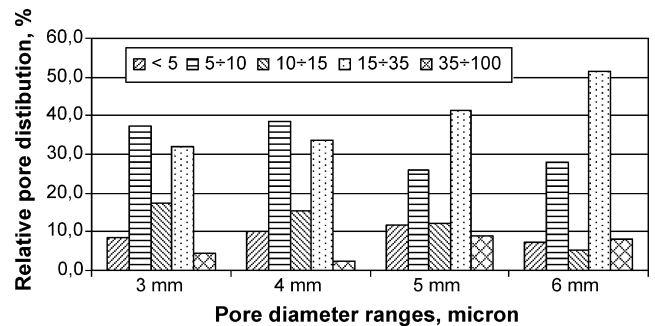
Fig. 8. Diagram collecting of pore size distribution of indicated samples for *n*=0.30 (at indicated ranges).

Fig. 9. Diagram collecting of pore size distribution of Type IIa samples in dependence on maximum grain size (at indicated ranges).

investigations utilized fused magnesia were conducted. The fused spinel content was 8% or 18%. Properties of Type IIIa and IIIb samples for different *n* values and for different maximum grain size in dependence on fused magnesia content are presented in Tables 7 and 8.

4. Conclusions

Presented results described the influence of sintered and fused magnesia with different morphology and physical-chemical properties on final properties of magnesia-spinel products containing 8 or 18 mass% of fused spinel. The main goal was the determination of technological conditions for manufacturing products with low gas permeability and open porosity.

The used magnesia raw materials have different the CaO/SiO₂ mole ratio. They differ in Fe₂O₃ content, the level of density, the size of periclase crystals (Table 1) and pore size

distribution (Fig. 1). The clinker 2 (sintered magnesite) showed the highest amount of pores smaller than $10\text{ }\mu\text{m}$. The fused magnesite contains the major part of pores bigger than $15\text{ }\mu\text{m}$. The used fused spinel has the pores bigger than $15\text{ }\mu\text{m}$, mainly (Fig. 1). The pore size distribution in raw materials surely influenced the microstructure evolution and pore size distribution in final products. This was also decisive for gas permeability of products.

It was shown that for each group of used raw materials it is possible to achieve a product with good properties. The products containing high amount of fused spinel, independently on kind of used magnesite, have high open porosity, gas permeability and low crushing strength. Products with low amount of fused spinel showed better properties.

Low gas permeability was connected with amount of pores smaller than $10\text{ }\mu\text{m}$. Such properties have products prepared with low coefficient n value for the same maximum grain size or the products with smaller maximum grain size prepared with the constant n value. The optimum useful properties were achieved for mixes with $n=0.22$ or 0.30 for given maximum grain size or for maximum grains size equal 4 or 5 mm for the constant n value.

The forming pressure of 160 MPa, allowed achieving a profitable level of densification at used firing temperatures.

During performed tests it was established that magnesite-spinel products derived from mixes containing sintered magnesite (clinker 2) and spinel reached the most profitable properties.

Acknowledgement

The work was partially financed by Polish State Committee for Scientific Research (Grant No. 3 T08D 009 26).

References

1. EN 12475-2, Classification of dense shaped refractory products. Part 2. Basic products containing less than 7% residual carbon, 1998.
2. Austria Patent No. 158208 (2 March 1932).
3. Kimura, M., Yasuda, Y. and Nishio, H., Development of magnesite spinel bricks for rotary cement kilns in Japan. *Interceram*, 1984(Special Issue), 22–28.
4. Bartha, P., Direktgebundene Periklasspinellsteine und ihr Einsatz in der Zementindustrie. *Zement Kalk Gips*, 1982, **9**, 500–508.
5. Bartha, P., Chemisch-mineralogische Charakterisierung ungebrauchter und gebrauchter feuerfester Steine auf der Basis $\text{MgO-Al}_2\text{O}_3$. *Zement Kalk Gips*, 1985, **2**, 96–99.
6. Muan, Osborne: Schlackenatlas. Verlag Stahleisen. mbH, Düsseldorf, 1981, p. 30.
7. O'Driscoll, M., Spinel review. *Industrial Minerals*, 1994, **324**, 35–49.
8. Bartha, P. and Klischat, H. J., Klassifikation von Magnesit-Steinen nach Spezifikation und Gebrauchswert im Zementdrehrohrofen. *Zement Kalk Gips*, 1994, **8**, 474–478.
9. Szczerba, J., Causes of changes in applying and development of spinel refractories for cement kilns. *Materiały Ogniotrwałe*, 1997, **2**, 59–66.
10. Ohno, M., Tokunaga, K., Tsuchiya, Y., Mizuno, Y. and Kozuka, H., Applications of chrome-free basic bricks to cement rotary kilns in Japan. In *Proceedings of the UNITECR'03*, 2003, pp. 27–30.
11. Klischat, H. J. and Bartha, P., Progress in performance behaviour of basic bricks by innovative raw material selection. In *Proceedings of the UNITECR'01*, 2001, pp. 631–641.
12. Szczerba, J. and Piech, J., Selected aspects of chemical corrosion of magnesite chromite and magnesite spinel refractories used in rotary cement kilns. *Cement Wapno Gips*, 1995, **4**, 110–116.
13. Ozeki, F., Tokunaga, K., Kozuka, H., Kajita, Y. and Honda, T., Study on refractories affected by utilization of leaching wastes in cement rotary kiln. In *Proceedings of the UNITECR'01*, 2001, pp. 669–684.
14. Kozuka, H., Kajita, Y., Tsuchiya, Y., Honda, T. and Ohta, S., New kind of chrome free (MgO-CaO-ZrO_2) bricks for burning zone of rotary cement kiln. In *Proceedings of the UNITECR'93*, 1993, pp. 1027–1037.
15. Kozuka, H., Kajita, Y., Tsuchiya, Y., Honda, T. and Ohta, S., Further improvements of MgO-CaO-ZrO_2 bricks for burning zone of rotary cement kiln. In *Proceedings of the UNITECR'95*, 1995, pp. 256–263.
16. Nievoll, J. and Buchberger, B., Performance of new chrome free magnesite bricks in precalciner kilns. *Veitsch-Radex Rundschau*, 1999, **1**, 57–64.
17. Klischat, H. and Weibel, G., Variation of physical and chemical parameters as a tool for development of basic refractory bricks. In *Proceedings of the UNITECR'99*, 1999, pp. 204–207.
18. Geith, M., Majcenovic, C. and Wiry, A., Hercynite & Galaxite—“Active Spinel. Additives for Excellent Cement Rotary Kiln Bricks”. *RHI Bulletin*, 2003, **1**, 25–28.
19. Komatsu, H., Arai, M. and Ukawa, S., Current and future status of chrome-free bricks for rotary cement kilns. *Taikabutsu Overseas*, 1999, **4**, 3–9.
20. Kaneyasu, A., Trends of basic refractory raw materials—magnesite aggregate for chrome-free bricks. *Journal of the Technical Association of Refractories, Japan*, 2000, **4**, 245–248.
21. Funk, J. E. and Dinger, D. R., Particulate size control for high-solids castable refractories. *American Ceramic Society Bulletin*, 1994, **73**, 66–69.